Biosystems Engineering (2005) **90** (4), 397–407
doi:10.1016/j.biosystemseng.2004.11.006
PM—Power and Machinery

The Evaluation of Close-range Photogrammetry for the Modelling of Mouldboard Plough Surfaces

M.A. Aguilar; F.J. Aguilar; F. Agüera; F. Carvajal

Departamento de Ingeniería Rural, Universidad de Almería, Escuela Politécnica Superior, La Cañada 04120, Almería, Spain; e-mail of corresponding author: maguilar@ual.es

(Received 26 April 2004; accepted in revised form 23 November 2004; published online 2 March 2005)

The geometric heterogeneity existing in mouldboard ploughs hinders its inclusion in models in which the redistribution of soil particles is predicted, or the force exerted on the working component is measured. In this study, both the mathematical surface (second-, third- and fourth-order polynomials, both splines and Bezier) and the number of control points required for its adjustment (100, 49, 25, 20, 16), are examined to produce optimal modelling of the mouldboard plough geometry. The three-dimensional coordinates of 193 points on the surface of a plough are measured with great accuracy (root mean square 0·66 mm), using low-cost close-range photogrammetry. The results obtained indicate that the surface of a mouldboard plough can be shaped with an accuracy of approximately 1·30 mm, with the adjustment of a cubic polynomial surface to just 25 control points randomly distributed over the surface of the plough.

1. Introduction

In modern agriculture, conservation of soil as a productive element is becoming more and more relevant, and for this reason care must be taken of vital aspects such as erosion processes due to the preparation of the soil through different operations. Within the tools employed by farmers, the mouldboard plough is among those which alter the original position of soil particles to a greater extent. Although the decrease in the use of mouldboard ploughs can reduce negative environmental effects, such as erosion or compactness of the soil (Soane & Van Ouwerkerk, 1994), this operation is still widely used in mechanised agriculture in many countries. The main reason is that this tillage operation is very efficient for improving soil structure, burying fertilisers and residues of the preceding crop and controlling weeds (Moss & Clarke, 1994).

Owing to the large variety of soil types and ploughing conditions, many different shapes of mouldboard have been developed: cylindrical, cylindroidal and helical. Ortiz-Cañavate (1993) classifies mouldboards in terms of their geometry (cylindrical, universal and warped) and with regard to their inclination (steep, semi-steep and distended). The geometrical heterogeneity existing in mouldboard ploughs hinders their inclusion in the models which try to predict the redistribution of soil particles or to measure the force exerted on the working component.

The determination of three-dimensional (3D) coordinates of points on the surface of the mouldboard plough is absolutely necessary for the modelling its geometric surface. In this study, an optical coordinate measuring technique is proposed for points situated on the surface of a mouldboard plough. Specifically, a low-cost digital close-range photogrammetric software package and digital consumer-grade camera are used. A non-contact 3D digitiser is utilised to evaluate the photogrammetric method. The non-contact 3D digitiser is the most accurate optical coordinate measuring method available at present. It is usually employed in Reverse Engineering.

The main objectives of this study are the following:

(1) to evaluate the accuracy in measuring the 3D coordinates of points on the surface of a mouldboard plough using close-range photogrammetry; and

(2) to study the simple mathematical surface which best fits the actual surface of the plough with the fewest control points, this surface can be applied to the theoretical analysis of the working process and the manufacture of the mouldboard.

2. Literature review

Various authors have worked on the geometric characterisation of the mouldboard plough. White (1918) suggested that many mouldboard ploughs could be adjusted to the equation of a hyperbolic paraboloid. Ortiz-Cañavate and Hernanz (1979) found that cubic polynomial equations explicit in coordinate z and without an independent term, were quite a good fit for a great number of mouldboard ploughs. Crăciun and Leon (1998) presented an analytical method to identify and design mouldboard plough surfaces with cylindroidal geometry. More recently, there are authors who use design surfaces for the geometric modelling of mouldboard ploughs, fundamentally, Bezier bicubic parametric surfaces (Richey *et al*., 1989; Ravonison & Destain, 1994; Gutiérrez de Ravé *et al*., 2002).

The measurement of the 3D coordinates of points on mouldboard plough surfaces has been done in various ways. Reed (1941) obtained coordinates with points belonging to the surface of the plough through direct measuring. For this purpose, he set a pair of boards pierced with a set of holes distributed in the shape of a reticule. These boards were placed parallel and vertical to each other, so that the nets of slits coincided. The position of each hole was defined by coordinates x and y. Coordinate z was measured using a cylinder which went through the corresponding orifices in each board until one of its sides touched the surface of the plough. Soehne (1959) projected a light through a slit, either horizontal or vertical, on to the painted plough surface. A camera was used to record the reflected light. A series of photographs was taken by moving the plough to different positions. The technique was useful to compare the shapes of different ploughs. Ravonison and Destain (1994) obtained 3D coordinates with points on the surface of the plough using a pantograph consisting of six kinematic links. More recently, Gutiérrez de Ravé *et al*. (2002) used a laser device to measure profiles on the mouldboard plough.

Close-range photogrammetry offers the possibility of obtaining the 3D coordinates of an object from two-dimensional (2D) digital images in a rapid, accurate, reliable, flexible and economical way. This makes it an ideal tool for precise industrial measurement (Fraser, 1993). Photogrammetric methods have been recently used for measurements in fluid physics experiments in space (Mass *et al*., 2002), underwater archaeological surveying (Green *et al*., 2002), monitoring the thermal deformation of steel beams (Fraser & Riedel, 2000), monitoring river channel and flume surfaces (Lane *et al*., 2001).

The methods of geometric modelling and defining of the surface of a mouldboard plough have varied. In recent decades, numerous research works have quantified and modelled the soil movement generated by the use of this type of plough (Lindstrom *et al*., 1992; Govers *et al*., 1994; Van Muysen *et al*., 2002; De Alba, 2003). The factors examined most frequently in these studies are work speed, its depth, the topography of the terrain and the type of soil. However, some of these erosion models could be improved including the geometry of the tillage implement used, as suggested by Van Muysen *et al*. (2000) and Van Muysen *et al*. (2002). Another important factor, which depends directly on the geometry of the mouldboard plough, is the determination of the 3D components of the force required to do the work (draught force, side force and vertical force). Many researchers have tried to optimise the design of the mouldboard plough in order to attain a lower consumption of power at work (Shoji, 2001, 2004; Shrestha *et al*., 2001). Other authors have developed models to predict the forces required to move the soil on the surface of the mouldboard (Quiong *et al*., 1986; Richey *et al*., 1989).

Roger-Estrade *et al*. (2001) model the vertical and lateral movement of weed seeds while working with the mouldboard plough, using basic geometric variables of the plough and the plough-share, such as depth and width. In general, the emergence possibilities of the seed decrease with depth (Dyer, 1995).

3. Materials and methods

3.1. *Close-range photogrammetric method*

The photogrammetric 3D coordinate determination is based on the co-linearity equation (*e.g*. Slama, 1980) which simply states that object point, camera projective centre and image point lie on a straight line. The determination of the 3D coordinates from a definite point is achieved through the intersection of two or more straight lines. Therefore, each point of interest should appear in at least two photographs (*Fig. 1*). Next, the steps followed to measure 3D coordinates in points situated on the surface of the mouldboard plough using the photogrammetric method proposed above are detailed.

3.1.1. *Circular markers*

Before taking the photographs, 193 targets were marked on the surface of a mouldboard plough. For this purpose, 12·5 mm diameter circular self-adhesive labels were used. The central part of these labels had a 3·5 mm diameter red circle, the rest being white. The labels were distributed spatially over the whole mouldboard plough (*Fig. 2*).

3.1.2. *Photography*

Three converging axis digital photographs were taken of each one of the mouldboard ploughs studied at a distance of 2 m and 100% overlap (*Fig. 2*). Thus, the coordinates of each target were calculated by the intersection of three rays with which redundancy is achieved and therefore, greater precision. Numerous authors choose the design of a close-range photogrammetric network formed by three images when carrying out photogrammetric close-range work (Fraser & Riedel, 2000; Mills *et al.*, 2001). The digital camera used was an Olympus Camedia C-2500L. The images were created in Joint Photographic Experts Group (JPEG) format with dimensions of 1712 by 1368 pixels. The Olympus Camedia C-2500L camera has a 17 mm image, charge coupled device (CCD) pick up element with which the pixel size of the digital images is 4·98 µm. The images were taken using the full-width setting of the camera zoom lens (focal length 9·3 mm). This means that the dimension of individual pixels in the object space or surface of interest is close to 1·07 mm. Some authors (Faig *et al.*, 1996; Deng & Faig, 2001) suggest that the non-metric photographs taken with digital cameras instead of analogical ones allow for higher precision in the calculation of coordinates by close-range photogrammetry.

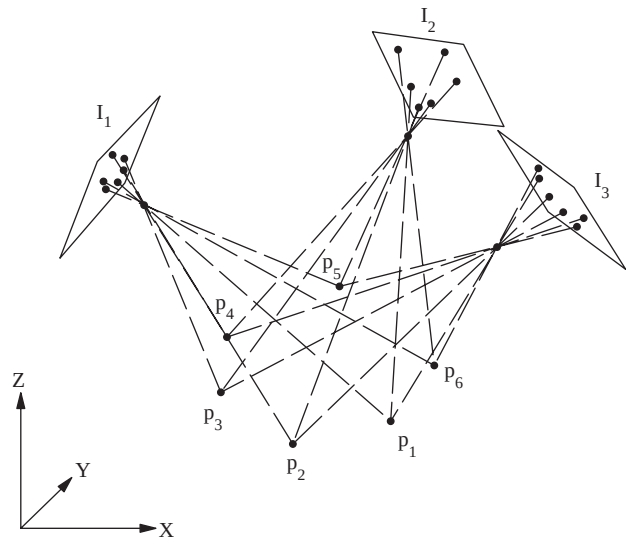

Fig. 1. Coordinate of object points (P_i) by triangulating bundles of observation rays from different image planes (I_i)

In order to have a set of known photogrammetric 3D coordinate control points, a white portable aluminium rectangular frame (1350 mm by 850 mm) was built. In it, 43 cylinders with variable heights between 2·5 and 200 mm were fitted. At the top of each cylinder, 43 photogrammetric control points were placed (3 mm diameter black dots) with known 3D coordinates. Using the left-hand corner of the frame as the origin for a local coordinate system, the X-axis coincided with the larger side of the rectangle, the Y-axis with the smaller side and the Z-axis was orientated according to the direction of the heights of the cylinders, perpendicular to the plane of the rectangle. The photogrammetric control points on the frame were surrounding the unknown targets on the mouldboard plough surface in each of the three images in the photogrammetric network (*Fig. 2*).

3.1.3. *Photogrammetric three-dimensional coordinates determination*

To obtain 3D coordinates for the 193 targets of the mouldboard plough surface a close-range photogram-

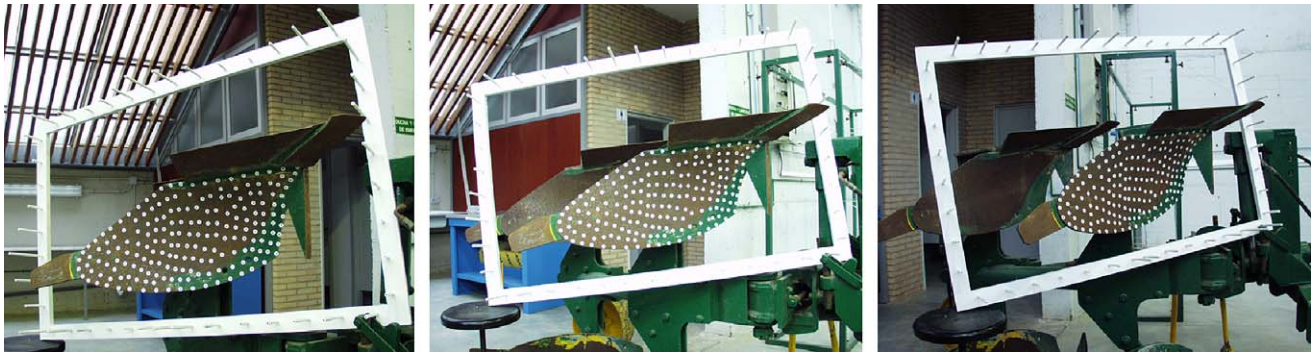

Fig. 2. Images used in the photogrammetric analysis; first mouldboard type of plough with 193 targets and the rectangular frame with photogrammetric control points

metric software package named ShapeCapture® (ShapeQuest Inc., Nepean, Canada) was used. This software has three infrastructures: calibration, registration and computation of 3D coordinates.

The objective of the calibration is to solve the external and internal parameters of the camera using known photogrammetric control points in the field of view. The internal parameters are focal length f, the x and y coordinates of the principal point of the image x_0 and y_0, image parameters honed to correct the scale difference and non-perpendicularity of the x and y image coordinates A and B, radial lens distortion parameters K_1 and K_2, and lens distortion parameters dislocating from the centre P_1 and P_2. The external parameters are the position and orientation of the camera when the image was taken. These are the coordinates of the camera projection centre x_c, y_c and z_c, and three rotation angles around the X-axis (pitch), the Y-axis (roll), and the Z-axis (yaw).

Calibration requires eight or more photogrammetric control points in the scenes where the coordinates are known in a 3D reference system. In our case, 22 photogrammetric control points belonging to the reference system and the image coordinates were used, of which were measured on the three images. Working with similar software to that used in our work, Deng and Faig (2001) used 24 photogrammetric control points to orientate a photogrammetric network.

Once the three photographs had been calibrated, the image coordinates of the 193 targets were marked on the surface of the plough, in each one of the three images, identifying which points in each image were the same as the physical points on the plough. This process is called 'referencing' the points. Subsequently, the registration to determine the position and orientation of each image relative to the reference coordinate system was completed. Registration is based on a photogrammetric bundle adjustment (Granshaw, 1980), through which a simultaneous solution to all image location and orientation and all the coordinates of the measured points are found. In those cases where a sufficient number of overlapped images are found with a sufficient number of common points, the number of equations is usually larger than the number of unknowns, thus a solution is possible. This is the main principle of the photogrammetric triangulation approach known as bundle adjustment. The system of equations to be solved is an over-defined non-linear system that requires an iterative solution. The initial values in the first iteration are those of the initial calibration of the images which are honed until the external parameters (of each image) are found as well as the internal ones (for the three images) which minimised errors in all the targets. This procedure gives the 3D coordinates of all the points used for registration.

3.2. *Measurement accuracy of the photogrammetric method*

Two trials were devised to estimate the accuracy of the method for the determination of points on the surface of the mouldboard plough using close-range photogrammetry.

3.2.1. *Grid points on a planar surface*

On a flat surface, 63 points were marked, distributed in the shape of a 100 mm by 50 mm mesh, with a total of nine rows and seven columns. Thus, the dimensions of the area covered by these points (700 mm by 450 mm), was similar to that occupied by the mouldboard plough. The mesh of points was printed in a plotter HP 1050C on acetate paper, which later was glued on a clear glass. The 3D coordinates of each point were calculated following the same methodology previously explained.

After obtaining the 3D coordinates of all the points marked on the flat surface, the point clouds was adjusted to a plane. Later the residuals in z of the 63 points were calculated by the difference between the coordinate z measured using photogrammetry and the one adjusted to the planar surface.

3.2.2. *Non-contact three-dimensional digitiser*

Another way of checking the 3D measurement accuracy of the close-range photogrammetric method was the comparison between the 3D coordinates of the 193 targets and a point cloud from the surface of the mouldboard obtained using more precise methods.

A Minolta Vidid 910 non-contact 3D laser digitiser was used to measure the 3D coordinates of the points on the surface of the mouldboard with great accuracy. Some technical specifications of this instrument are presented in Table 1.

The points were measured at a distance of 1 m, using a lens with a focal length of 25 mm. The maximum surface that could be digitised was 188 mm by 141 mm from which a cloud of 640 by 480 points was obtained. In order to obtain the points cloud of the total surface of the mouldboard, it was necessary to measure 10 patches of it with overlaps. These were joined using the software RapidForm® (INUS Technology Inc., Seoul, Korea) generating a complete model formed by 1 500 000 3D points. This same program was used to align the 193 targets measured by close-range photogrammetry and the point cloud obtained with the laser system. Thus, both the mistakes made using the photogrammetric system and their distribution were estimated.

Table 1
Technical specifications of the three-dimensional (3D) laser digitiser

Model name	Non-contact 3D digitiser VIDID 910/VI-910
Measurement method	Triangulation, light-stripe method
Accuracy, mm	
x	$\pm 0{\cdot}22$
y	$\pm 0{\cdot}16$
z	$\pm 0{\cdot}10$
Precision, mm	0·008
Output data points	3D data: 640×480

3.3. *Adjustment of analytical surfaces*

The second objective of this study was to find a geometric surface which could be adjusted as accurately as possible to the targets measured on the mouldboard plough surface. Defining this surface using a simple mathematical equation allows for the easy integration of the geometry of the plough in tillage erosion models, weed seed movements or reaction force analysis models. It was moreover, necessary to quantify the lowest number of control points which make a good fit, so that the cost of collecting data would go down.

To this end, a random sample was taken of 50 checkpoints from the 193 targets measured on the surface of the mouldboard plough. These checkpoints were used to carry out a true validation (Voltz & Webster, 1990). From the 143 remaining points, sub-samples of 100, 49, 25, 20 and 16 points were drawn. In the 20 and 16 point sub-samples, 10 points were taken randomly from the edge of the mouldboard and the rest from the inside, while the other samples were drawn totally at random. This action was carried out on four occasions, thus obtaining different combinations.

Adjustments were tested with explicit polynomial surfaces in z, quadratic ones (six coefficients), cubic ones (10 coefficients) and fourth-order ones (15 coefficients). Likewise, adjustments to design surfaces, such as Bezier or splines were also investigated. Among the first, Bezier bicubic parametric surfaces were chosen [Eqn (1)] where u and v are parameters with values limited to $0 \leqslant u \leqslant 1$ and $0 \leqslant v \leqslant 1$, $\bar{\boldsymbol{r}}(u, v)$ are the position vectors of any point on the surface and $\bar{\boldsymbol{r}}_{ij}$ are position vectors of control points.

$$\bar{\boldsymbol{r}}(u,v) = \sum_{i=0}^{3}\sum_{j=0}^{3} \bar{\boldsymbol{r}}_{ij} \frac{3!}{(3-i)!i!}\frac{3!}{(3-j)!j!} \times u^i(1-u)^{3-i}v^j(1-v)^{3-j} \quad (1)$$

For the adjustments of the mouldboard point sub-samples to spline surfaces [Eqn (2)], the development proposed by Yu (2001) is used

$$z(x,y) = a_0 + a_1 x + a_2 y + \sum_{i=0}^{N} F_i r_i^2 \ln(r_i + \varepsilon)^2$$

$$\sum_{i=0}^{N} F_i = 0, \quad \sum_{i=0}^{N} x_i F_i = 0, \quad \sum_{i=0}^{N} y_i F_i = 0,$$
$$r_i^2 = (x - x_i)^2 + (y - y_i)^2 \quad (2)$$

where: N is the number of control points (x_i, y_i, z_i, $i = 1, 2 \ldots, N$); $F_i\,(i = 1, 2, \ldots, N)$, a_0, a_1 and a_2 are $N + 3$ coefficients, and the parameter ε is a small quantity, which is usually taken to be between 10^{-2} and 10^{-6}, depending on the degree of the curvature variation of the surface.

Once the analytical surfaces that best fitted each of the repetitions had been obtained using the different control point sub-samples, the residuals were defined in the 50 checkpoints chosen initially.

This methodology was used for the points measured with the non-contact 3D laser digitiser, although in this case only third- and fourth-order polynomial surfaces were considered.

The results obtained in the statistical analysis of the data generated in the first mouldboard, were validated with two further ploughs, the shapes and sizes of which were very different. In each of these ploughs, a total of 100 targets were measured on this occasion in order to choose the four repetitions.

3.4. *Statistical analysis*

To determine the analytical surface and the optimal number of necessary points for the adjustment which was defining in a more precise way the mouldboard plough, the residuals generated were analysed.

The checkpoint residuals in the root mean square of z (RMS_z) [Eqn (3)] and their maximum residual ($R_{\max}$) were the variables observed in the analysis of variance with factorial model and four repetitions (Snedecor & Cochran, 1980). The variation sources analysed were the surfaces studied (SURF), the number of control points used in the adjustment (NPO) and the interaction between them (SURF by NPO). When the results of the analysis of variance were significant, the comparison of means was carried out using the Duncan multiple range tests, with a 95% confidence interval. The RMS_z is given by

$$E_z = \sqrt{\frac{\sum_{i=1}^{50} (z_i^{estimated} - z_i^{observed})^2}{50}} \quad (3)$$

where E_z is the root mean square error in z.

4. Results and discussion

4.1. *Measurement accuracy of photogrammetric method*

The two trials carried out to evaluate the accuracy of the photogrammetric method showed very similar results. Table 2 shows some statistics related to the residuals population in z, expressed in the absolute value obtained in both trials. The coincidence between the statistics of both absolute error populations makes the results obtained very reliable.

On the other hand, in *Fig. 3* one sees that the distribution of absolute errors when comparing point clouds obtained with close-range photogrammetry with a 3D laser digitiser is totally random.

The adjustment to a plane of the 63 targets measured on a crystal surface showed a high coefficient of multiple determination ($R^2 = 0{\cdot}998$). In Table 2, one can see that the value of RMS_z is about 0.66 mm, approximately 2/3 of the size of a pixel. The relative error with regard to the size of the photographed object is 1/2400, considering as maximum dimension of the object the diagonal of the reference system rectangular frame. The relative errors found in the bibliography are very variable. Deng and Faig (2001) obtained relative errors of 1/1635 and 1/1684 working with two different digital cameras (Kodak CD-50 and Fujix DS-100) on two different scales, whilst with one Olympus OM, 35 mm camera the relative errors were 1/781. On the other hand, Fraser and Riedel (2000) obtained relative errors of 1/9000 with similar photogrammetric software to the one employed in our work and with three digital cameras of the same model used simultaneously.

Table 2
Descriptive statistics of the absolute values of the residuals in coordinate z generated in the trials to evaluate the accuracy of the photogrammetric method

	Trial 1	*Trial 2*
Mean, mm	0·50	0·51
Standard deviation, mm	0·40	0·41
Minimum value, mm	0	0
Maximum value, mm	1·86	1·76
Root mean square error in z (RMS_z), mm	—	0·66

Trial 1, adjustment to a planar surface; trial 2, comparison with the three-dimensional (3D) laser digitiser.

The accuracy attained with the photogrammetric systems will vary in terms of factors such as the resolution of the photograph, the type and quality of the camera, the number of photographs, the design of the photogrammetric network and the number of referenced points. The desired precision p is related, among other things, to the dimension of individual pixels in the object space d_o, so that approximately: $p \approx d_o$. The dimension of a pixel on the object is controlled by the scale of the photograph (f/D, where f is the focal length and D is the distance between the camera and object) and the physical size of the pixel in the image space d_e. Thus, the expected precision of derived elevations is given by Eqn (4):

$$p \approx d_o = \frac{d_e}{f/D} \tag{4}$$

In a previous study, Mills *et al.* (2001) obtained RMS_z values of 1·38 and 1·15 mm in 55 checkpoints measured with two different photogrammetric software packages. The photogrammetric network was formed by three photographs taken with a Wild P32 metric camera at a distance of 2·5 m and with a pixel size on the photographed object of 1·1 mm. Lane *et al.* (2001) obtained 1·5 mm RMS_z working with a Kodak DCS460 digital camera and with a pixel size on the object of 0·6 mm. On the other hand, values for RMS_z of approximately 1/3 of a pixel obtained by Pappa *et al.* (2001) in 521 checkpoints, using Kodak DC290 con-

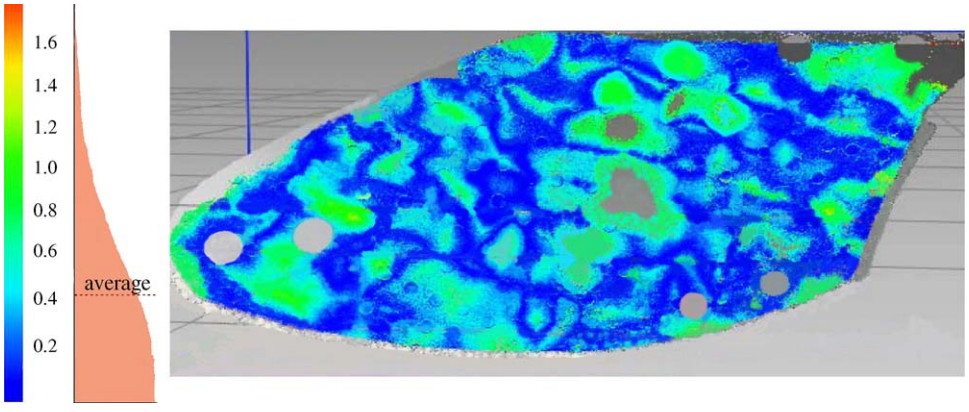

Fig. 3. Discrepancies in absolute values between the point clouds obtained by close-range photogrammetry and with the three-dimensional (3D) laser digitiser; the histogram values of the residuals are expressed in mm

sumer digital cameras and Photomodeler Pro software package (Eos Systems Inc., Vancouver, Canada). With the same software and a Fujifilm MX-2900 digital camera, Fedak (2001) obtained values for RMS_z of around 1/4 of a pixel in 54 checkpoints.

The values for RMS_z of 0·664 mm and R_{max} of 1·85 mm estimated in our study for the photogrammetry close-range method employed would be adequate for the geometric modelling of mouldboard ploughs.

4.2. *Analytical surface adjustment*

The Bezier bicubic parametric surface was the one that fitted worst the mouldboard plough geometry. In Table 3 the mean results and the standard deviations are presented for the four RMS_z combinations and the R_{max}. These results were obtained when the control point sub-samples (100, 49, 36, 25 and 16) and the 50 checkpoints were measured by close-range photogrammetry. The Bezier surfaces fitted always underestimated the value of coordinate z measured on the surface of the plough, so that the residuals generated were always negative. The explanation for this fact can be seen in a schematic way by reducing the problem to two dimensions (*Fig. 4*). One must bear in mind that the Bezier curves only go past the first and last control point (P_0 and P_3) and are tangential to its initial and final sides.

To obtain a value for the RMS_z of less than 2 mm, it would be necessary to adjust the Bezier surface using a control point number which is higher than 100. Ravonison and Destain (1994) propose an iterative selection method of control points for the adjustment of Bezier parametric cubic surfaces. The main variation is that these control points need not belong to the plough surface. This method needs 24 measured points on the edge of the mouldboard plough. Using this method,

Table 3
Adjustment of the control point sub-samples measured by close-range photogrammetry to Bezier surfaces

Number of control points (NPO)	*Root mean square error in z (RMS_z), mm*		*Maximum residual in z (R_{max}), mm*	
	Mean	*SD*	*Mean*	*SD*
16	14·62	1·01	−20·96	1·22
25	11·07	0·53	−16·73	2·18
36	8·96	0·68	−14·79	3·23
49	7·48	0·44	−11·52	0·84
100	4·37	0·35	−8·42	0·72

Mean and standard deviation (SD) of the checkpoint residuals in the z root mean square error (RMS_z) and maximum residual error (R_{max}) obtained for the four combinations investigated.

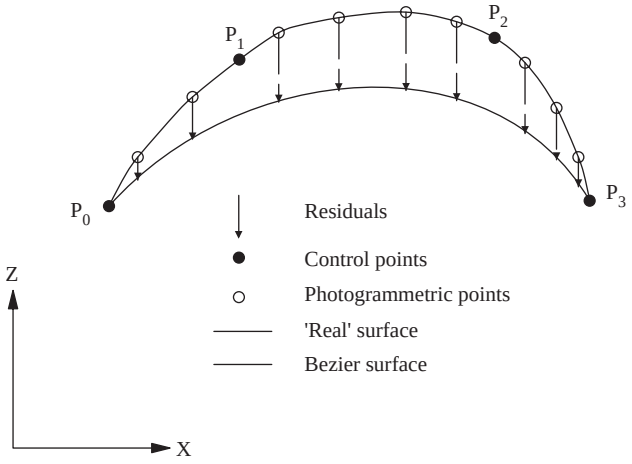

Fig. 4. Bidimensional diagram illustrating the underestimation of the z values in the Bezier bicubic parametric surfaces

values were obtained for R_{max} of 1·90 mm and for RMS_z of 1·63 mm, although these values were calculated only on nine checkpoints. Later on, Gutiérrez de Ravé *et al.* (2002) used the algorithm developed by Ravonison and Destain (1994) with the purpose of carrying out an evaluation of their quality, obtaining a value for RMS_z of 8·94 mm calculated in 121 checkpoints.

In Table 4, the analysis of variance for RMS_z with 3D points obtained with close-range photogrammetry is presented. Polynomials of second (P-2), third (P-3) and fourth order (P-4) as well as splines surfaces (SP) were used. As to the control points, the 16-point sub-samples were eliminated from the analysis of variance since it produced extremely poor fits in certain repetitions of third- and fourth-order polynomial surfaces. One can observe how the type of surface used in the fit (SURF), the number of control points (NPO) and the interaction of both (NPO × SURF) have a significant influence (probability $P<0·05$) on the RMS_z (SURF > NPO > SURF × NPO). Something very similar occurs when the R_{max} is analysed as the dependent variable.

The separation of means (Table 5) shows us how P-3 and P-4 polynomial surfaces are the ones which present the best fits, with values for RMS_z of 1·33 and 1·18 mm respectively, and with no significant differences ($P<0·05$) between them. As to the variation source NPO, the RMS_z for the adjustments with 100, 49 and 25 points do not present significant differences ($P<0·05$).

In Table 6, the separations of means for SURF and NPO are presented, both for RMS_z and for R_{max}. With regard to the P-2 and P-4 surfaces, there are no significant differences ($P<0·05$) due to NPO, whereas for the P-3 and SP surfaces the lower value of NPO which cannot separate significantly ($P<0·05$) is 25 points. With regard to R_{max}, the NPO variation source

Table 4
Analysis of variance table for root mean square error in z (RMS_z) of photogrammetric residuals

Source	*Degree of freedom*	*Sum of square*	*Mean square*	*F-test*	*Probability*
Number of control points (NPO)	3	17·73	5·91	9·17	$P<0·01$
Shape of surface (SURF)	3	47·98	15·99	24·82	$P<0·01$
Interaction (NPO × SURF)	9	12·80	1·42	2·21	0·038
Residual	48	30·92	0·64		
Total	63	109·43			

Table 5
Comparison of root mean square error in z (RMS_z) means by shape of surface (SURF) and number of control points (NPO) using photogrammetric points

Shape of surface (SURF)	*RMS_z, mm*	*Number of control points (NPO)*	*RMS_z, mm*
Second-order polynomial (P-2)	$3·35^{a}$	20	$2·87^{a}$
Spline (SP)	$2·23^{b}$	25	$2·02^{b}$
Third-order polynomial (P-3)	$1·33^{c}$	49	$1·69^{b}$
Fourth-order polynomial (P-4)	$1·18^{c}$	100	$1·50^{b}$

Values of the same column followed by different superscript letters indicate significant differences at a probability level $P<0·05$; P-2, P-3 and P-4, second-, third- and fourth-order polynomial surfaces; SP, spline surface.

Table 6
Comparison of the root mean square error in z (RMS_z) and maximum residual (R_{max}) means by shape of surface (SURF) and number of control points (NPO) using photogrammetric points

Number of control points (NPO)	*Root mean square error in z (RMS_z), mm*				*Maximum residual (R_{max}), mm*			
	Shape of surface				*Shape of surface*			
	P-2	*P-3*	*P-4*	*SP*	*P-2*	*P-3*	*P-4*	*SP*
20	3·64	$1·64^{b}$	1·96	$4·25^{b}$	8·72	4·04	4·66	$11·64^{b}$
25	$3·39_{c}$	$1·30^{ab}_{a}$	$1·07_{a}$	$2·33^{ab}_{b}$	$9·02_{b}$	$2·93_{a}$	$2·66_{a}$	$6·60^{ab}_{b}$
49	$3·22_{c}$	$1·21^{ab}_{ab}$	$0·88_{a}$	$1·44^{ab}_{b}$	$8·68_{c}$	$2·92_{ab}$	$2·17_{a}$	$4·24^{a}_{b}$
100	$3·14_{c}$	$1·16^{a}_{b}$	$0·79_{a}$	$0·89^{a}_{ab}$	$8·53_{b}$	$2·79_{a}$	$2·00_{a}$	$2·20^{a}_{a}$

Different subscript letters within the same row indicate significant differences at a probability level $P<0.05$; different superscript letters in the same column indicate significant differences at $P<0·05$; P-2, P-3 and P-4, second-, third- and fourth-order polynomial surfaces; SP, spline surface.

only has a clear influence on the SP surface, without statistical differences among the 100, 49 and 25 point samples. When NPO is equal to 25 points, the surfaces that best fit the mouldboard plough are P-3 and P-4 both for RMS_z and for R_{max}.

From the statistical analysis carried out with the points measured using close-range photogrammetry, it has been concluded that with a value for NPO of 25 one can obtain values for RMS_z and R_{max}, which at a reliability interval of 95% are as good as for NPO of 49 or 100. However, with regard to the choice of surface, any different between P-3 and P-4 was found. A more detailed analysis of the behaviour of the RMS_z and R_{max} for these surfaces with regard to NPO and using 3D points measured with the laser digitiser can be seen in Table 7. In this table, no significant differences ($P<0·05$) between the two surfaces, except for RMS_z with NPO equal to 100 points, were found. The RMS_z obtained with the 3D laser digitiser in the P-3 and P-4 surfaces and for NPO of 25 was reduced by 0·50 and 0·42 mm with regard to the values presented in Table 6, measured with photogrammetry. These values coincide approximately with the differences in accuracy estimated between the two measuring methods (photogrammetric method RMS_z of 0·66 mm in Table 2, 3D laser z accuracy of 0·10 mm in Table 1).

The great difference in price of the equipment required for the application of the two optical techniques used in this study for measuring the coordinates must take into consideration. The total cost of the digital camera and the software used in the method for measuring points with close-range photogrammetry is under 2000 Euros. On the other hand, the 3D laser digitiser and the software required for data handling cost over 100 000 Euros.

The number of points needed to shape a mouldboard plough will have an influence on the cost and the efficiency of the process. Stone and Gulvin (1977) considered that 250 points were necessary to characterise a mouldboard. Ortiz-Cañavate and Hernanz (1979) measured more than 700 points in each of the 22 mouldboard ploughs they examined in their study. Only in studies where design surfaces have been used (Richey *et al*., 1989; Ravonison & Destain, 1994; Gutiérrez de Ravé *et al*., 2002), the number of control points was smaller, although the accuracies obtained were not very good. In our case, a suitable modelling of the mouldboard plough using only 25 control points and a cubic polynomial surface was achieved. The fourth-order polynomial surface was discarded due to its greater complexity and the great variation in the results obtained in different combinations.

5. Validation of results

The method proposed to characterise the geometry of the mouldboard plough using close-range photogrammetry and adjusted polynomial surfaces with 25 control points, has been applied to two mouldboard ploughs.

The results obtained in RMS_z and R_{max} (Table 8) are somewhat higher than those presented for the first mouldboard with NPO of 25 (Table 6). It must be borne in mind that photographs of the first mouldboard were taken in the laboratory, whereas the two new mouldboards were photographed in field conditions (*Fig. 5*), therefore the different positions of the camera, its distance from the object and the lighting conditions were not ideal. In any case, the results are still acceptable for the geometric modelling of mouldboard ploughs and confirm the results obtained for the first mouldboard.

6. Conclusions

(1) Of the analytical surfaces examined in this study, the ones presenting the best statistical fit with the three-dimensional (3D) points measured on

Table 7
Comparison of the root mean square error in z (RMS_z) and maximum residual (R_{max}) means by shape of surface (SURF) and number of control points (NPO) using 3D laser digitiser points

Number of control points (NPO)	*Root mean square error in z (RMS_z), mm*		*Maximum residual (R_{max}), mm*	
	Shape of surface		*Shape of surface*	
	P-3	*P-4*	*P-3*	*P-4*
20	$0{\cdot}90^{b}$	0·81	$2{\cdot}12^{b}$	1·96
25	$0{\cdot}80^{ab}$	0·64	$1{\cdot}69^{ab}$	1·46
49	$0{\cdot}72^{ab}$	0·59	$1{\cdot}60^{ab}$	1·32
100	$0{\cdot}60^{a}_{a}$	$0{\cdot}45_{b}$	$1{\cdot}26_{a}$	1·02

Different subscript letters within the same row indicate significant differences at a probability level $P<0{\cdot}05$; different superscript letters in the same column indicate significant differences at $P<0{\cdot}05$; P-3 and P-4, third- and fourth-order polynomial surfaces.

Table 8
Root mean square error in z (RMS_z) and maximum residual (R_{max}) obtained in the second and third mouldboard type (M-2 and M-3) with P-2, P-3 and P-4 polynomial surfaces and NPO of 25

Mouldboard type	*Root mean square error in z (RMS_z), mm*			*Maximum residual (R_{max}), mm*		
	Shape of surface			*Shape of surface*		
	P-2	*P-3*	*P-4*	*P-2*	*P-3*	*P-4*
M-2	$5{\cdot}23_{a}$	$1{\cdot}56_{b}$	$1{\cdot}22_{b}$	$13{\cdot}18_{a}$	$3{\cdot}82_{b}$	$2{\cdot}99_{b}$
M-3	$4{\cdot}65_{a}$	$1{\cdot}83_{b}$	$1{\cdot}62_{b}$	$11{\cdot}12_{a}$	$4{\cdot}46_{b}$	$3{\cdot}81_{b}$

Values in the same row followed by different subscript letters indicating significant differences at $P<0{\cdot}05$.

Fig. 5. Photographs taken of the second type (left = M-2) and third type (right = M-3) mouldboards

the surface of the mouldboard plough were fourth order and cubic polynomial surfaces. This fact was independent of the measuring method employed, close-range photogrammetry or 3D laser digitiser. Of the two, the cubic surfaces was favoured due to their greater simplicity, which makes them more adequate for participating in more complex erosion or force studies models. Moreover, the results obtained in the cubic polynomial surfaces present a lower variability for the different combinations investigated.

(2) The minimal number of control points required to achieve a good fit of the cubic surface was 25, randomly distributed. Appropriate accuracies for the analytical modelling of a mouldboard plough was obtained [root mean square error of the z coordinate (RMS_z) of 1·30 mm; maximum residual (R_{max}) of 2·93 mm] using cubic surfaces with 25 control points and low-cost measuring methods, such as close-range photogrammetry with consumer-grade digital cameras.

(3) Using more precise techniques to measure coordinates, such as a 3D laser digitiser, although it is more expensive, the goodness of the fit was considerably improved (RMS_z of 0·80 mm; R_{max} of 1·69 mm). The decrease in the RMS_z obtained with the laser digitiser with regard to the photogrammetric method coincides approximately with the differences in accuracy estimated between the two measuring methods.

(4) Close-range digital photogrammetry is an accurate, reliable, flexible and economical coordinate measurement technique. With the methodology described in this study very high accuracies have been achieved in the measurement of 3D (RMS_z of 0·80 mm; R_{max} of 1·69 mm). These values make it possible to use this technique in the modelling of numerous surfaces of agricultural interest.

Acknowledgements

We would like to thank the Centro Tecnológico Andaluz de la Piedra (CTAP) for all their assistance and for giving us the opportunity to use their non-contact 3D digitiser VI-910 and RapidForm 2004® in this study.

References

Crăciun V; Leon D (1998). An analytical method for identifying and designing a moldboard plow surface. Transactions of the ASAE, **41**(6), 1589–1599

De Alba (2003). Simulating long-term soil redistribution generated by different patterns of mouldboard ploughing in landscapes of complex topography. Soil and Tillage Research, **71,** 71–86

Deng G; Faig W (2001). An evaluation of an off-the-shelf digital close-range photogrammetric software package. Photogrammetric Engineering and Remote Sensing, **67**(2), 227–233

Dyer W (1995). Exploiting weed seed dormancy and germination requirements through agronomic practices. Weed Science, **43,** 498–503

Faig W; El-Habrouk H; Li X P; Hosny M (1996). A comparison of the performance of digital and conventional non-metric cameras for engineering applications. International Archives of Photogrammetry and Remote Sensing, **31**(Part B5), 147–151

Fedak M (2001). 3D measurement accuracy of a consumer-grade digital camera and retro-reflexive survey targets. http://www.photomodeler.com/pmpro07.html, accessed March 21, 2004

Fraser C S (1993). A resume of some industrial applications of photogrammetry. ISPRS Journal of Photogrammetry and Remote Sensing, **48**(3), 12–23

Fraser C S; Riedel B (2000). Monitoring the thermal deformation of steel beams via vision metrology. ISPRS Journal of Photogrammetry and Remote Sensing, **55,** 268–276

Govers G; Vandaele K; Desmet P; Poesen J; Bunte K (1994). The role of tillage in soil redistribution on hillslopes. European Journal Soil Science, **45,** 469–478

Granshaw S I (1980). Bundle adjustment methods in engineering photogrammetry. Photogrammetric Record, **10**(56), 181–207

Green J; Matthews S; Turanli T (2002). Underwater archaeological surveying using PhotoModeler, VirtualMapper: different applications for different problems. The International Journal of Nautical Archaeology, **31**(2), 283–292

Gutiérrez de Ravé E; Giráldez J V; Agüera J; Gil J (2002). Caracterización geométrica de aperos de labranza mediante métodos de aproximación sencillos. XIV Congreso Internacional de Ingeniería Gráfica, Santander (España), pp 84–90.

Lane S N; Chandler J H; Porfiri K (2001). Monitoring river channel and flume surfaces with digital photogrammetry. Journal of Hydraulic Engineering, **127**(10), 871–877

Lindstrom M J; Nelson W W; Shumacher T E (1992). Quantifying tillage erosion rates due to mouldboard plowing. Soil and Tillage Research, **24,** 243–255

Mass H G; Virant M; Becker J; Bösemann W; Gatti L; Henrichs A (2002). Photogammetric methods for measurements in fluid physics experiments in space. Acta Astronautica, **50**(4), 225–231

Mills J P; Newton I; Peirson G C (2001). Pavement deformation monitoring in a rolling load facility. Photogrammetric Record, **17**(97), 7–24

Moss S R; Clarke J (1994). Guidelines for the prevention and control of herbicide resistant black-grass (*Alopecurus myosuroides*, Huds.). Crop Protection, **13,** 381–386

Ortiz-Cañavate J (1993). Las máquinas agrícolas y su aplicación. [The Agricultural Machines and their Applications.]. Mundi-Prensa, Madrid

Ortiz-Cañavate J; Hernanz J L (1979). Clasificación geométrica de las vertederas. [Geometrical classification of mouldboard.]. Anales del INIA Serie Tecnología Agrícola, **5,** 7–27

Pappa R S; Giersch L R; Quagliaroli J M (2001). Photogrammetry of a 5 m inflatable space antenna with consumer-grade digital cameras. Experimental Techniques, **25**(4), 21–29

Quiong G; Pitt R E; Ruina A A (1986). Model to predict soil forces on the plough mouldboard. Journal of Agricultural Engineering Research, **35**(3), 141–155

Ravonison N M; Destain M F (1994). Parametric cubic equations for modelling mouldboard plough surfaces. Soil and Tillage Research, **31,** 363–373

Reed I F (1941). Test of tillage tools: III. Effect of shape on the draft of 14-inch moldboard plow bottoms. Agricultural Engineering, **22,** 101–104

Richey S B; Srivastava A K; Segerlind S L (1989). The use of three dimensional computer graphics to design mouldboard plough surfaces. Journal of Agricultural Engineering Research, **43,** 245–258

Roger-Estrade J; Colbach N; Leterme P; Richard G; Caneill J (2001). Modelling vertical and lateral weed seed movements during mouldboard ploughing with a skim-coulter. Soil and Tillage Research, **63,** 35–49

Shoji K (2001). Design of a model 'Spot Plough' for inversion of the soil slice within the furrow. Journal of Agricultural Engineering Research, **79**(3), 283–297

Shoji K (2004). Forces on a model 'Spot Plough'. Biosystems Engineering, **87**(1), 39–45

Shrestha D S; Singh G; Gebresenbet G (2001). Optimizing design parameters of a mouldboard plough. Journal of Agricultural Engineering Research, **78**(4), 377–389

Slama C C (1980). The Manual of Photogrammetry, 4th Edn. American Society of Photogrammetrists, Falls Church, VA

Snedecor G W; Cochran W G (1980). Statistical Methods, 7th Edn. The Iowa State University Press, Ames, IA

Soane B D; Van Ouwerkerk C (1994). Soil compaction problems in world agriculture. In: Evaluation of Soil Organic Matter Models (Soane B D; Van Ouwerkerk C, eds), pp 181–199. Springer, Berlin

Soehne W (1959). Investigations on the shape of plough bodies for high speeds. Grundlagen der Landtechnik, **11,** 22–39

Stone A A; Gulvin H E (1977). Machines for Power Farming, 3rd Edn. Wiley, New York

Van Muysen W; Govers G; Van Oost K (2002). Identification of important factors in the process of tillage erosion: the case of mouldboard tillage. Soil and Tillage Research, **65,** 77–93

Van Muysen W; Govers G; Van Oost K; Van Rompaey A (2000). The effect of tillage depth, tillage speed and soil condition on chisel tillage erosivity. Journal of Soil and Water Conservation, **55,** 354–363

Voltz M; Webster R (1990). A comparison of kriging cubic splines and classification for predicting soil properties from sample information. Journal of Soil Science, **41,** 473–490

White E A (1918). A study of the plow bottom and its action upon the furrow slice. The Journal of Agricultural Research, **12,** 149–182

Yu Z W (2001). Surface interpolation from irregularly distributed point using surface splines, with Fortran program. Computers and Geosciences, **27,** 877–882